

Temperature- and magnetic-field-induced phase transitions in Fe-rich FePt alloys

Chuan-Bing Rong^{a)} and J. Ping Liu

Department of Physics, University of Texas at Arlington, Arlington, Texas 76019

(Received 29 January 2007; accepted 8 May 2007; published online 1 June 2007)

Structural and magnetic properties of the $\text{Fe}_x\text{Pt}_{100-x}$ ($x=78-88$) alloys have been investigated. It is found that for all of the investigated compositions, a phase transition occurs from the disordered γ phase to the ordered α phase during cooling, while a reverse process takes place during heating. Moreover, magnetic fields also induce a phase transition from the γ phase to the α phase near the transition temperature. The temperature- and magnetic-field-induced phase transitions give rise to a huge negative thermal expansion and thus a giant magnetic entropy change (up to 39.8 J/kg K for the alloy with $x=79$). The contribution of the magnetic field induced phase transition to the total magnetic entropy change is estimated to be around 20%–25%. © 2007 American Institute of Physics. [DOI: 10.1063/1.2745255]

FePt alloys have attracted tremendous attention due to their richness in structures and magnetic properties. For instance, the equal atomic $L1_0$ FePt phase has potential applications in magnetic recording media and advanced permanent magnetic materials and the Fe_3Pt phase is a good Invar alloy. However, the structures and magnetic properties of the Fe-rich $\text{Fe}_x\text{Pt}_{100-x}$ ($x > 78$) alloys have rarely been systematically studied even it was reported 50 years ago that they undergo a first-order phase transition from the disordered γ phase with face-centered-cubic (fcc) structure to ordered α phase with body-centered-cubic (bcc) structure on cooling, and a reverse process on heating,¹⁻³ accompanied by a magnetization jump.⁴ The coupled structural and magnetic phase transitions are similar to those of recently developed materials with giant magnetocaloric effect (GMCE), such as FeRh,⁵ $\text{Gd}_5\text{Si}_4-x\text{Ge}_x$,⁶ $\text{LaFe}_{11.2}\text{Co}_{0.7}\text{Si}_{1.1}$,⁷ and $\text{MnFeP}_x\text{As}_{1-x}$,⁸ which undergo first-order phase transitions.^{9,10} Unlike a typical second-order magnetic transition, a first-order phase transition is always accompanied by unusual magnetic behavior such as coexistence of ferromagnetic and paramagnetic phases, a field- and temperature-induced reversible magnetic, and crystallographic phase transition. In this letter, we report a giant magnetic entropy change near room temperature which is related to a temperature- and magnetic-field-induced structural phase transition in the Fe-rich FePt alloys.

The $\text{Fe}_x\text{Pt}_{100-x}$ ($x=78-88$) alloys were prepared by arc melting by using 99.97% Fe and 99.9% Pt, followed by annealing for 48 h at 1373 K for homogenization. The weight loss during melting was negligible and therefore the initial composition is assumed to be unchanged. The compositions were also checked by energy dispersive x-ray analysis. The structure was determined by x-ray diffraction (XRD) with Cu $K\alpha$ radiation. The magnetization measurements were carried out with a superconducting quantum interference device magnetometer up to 7 T. High-temperature thermomagnetic curves were measured in a high-temperature oven in a physical property measurement system.

Figure 1 gives the thermomagnetic curves of the $\text{Fe}_{80}\text{Pt}_{20}$ alloy under 100 Oe as an example. First, the sample was heated to 950 K, at which the disordered γ phase was ob-

tained, then the sample was cooled down to 5 K before heating up again to 950 K at the rate of 10 K/min. A huge thermal hysteresis was observed as shown in Fig. 1. The thermal hysteresis is attributed to the phase transition from the disordered γ phase to the ordered α phase during cooling at the low temperature, while a reverse process took place during heating at relatively higher temperature.¹⁻³ Normally, the temperature region during phase transition is only several kelvins for the first-order transition systems such as GdGeSi and MnAsSb compounds.^{9,10} However, it is interesting to note that this region is as large as 30–40 K for the FePt system, as shown in Fig. 1, which should be attributed to the strong composition dependence of the transition temperature. The inset of Fig. 1 shows the composition dependence of the transition temperatures $T^{\alpha-\gamma}$ and $T^{\gamma-\alpha}$ during cooling and heating, respectively. It should be noted that the values were determined from the intersection of extrapolations of the greatest slope and flat region of the thermomagnetic curves. As one can see, the 1% compositional fluctuation can induce more than 50 K change in phase transition temperature especially when $x \leq 80$. The Fe content less than 78 leads to a disappearance of the thermal hysteresis due to the formation of Fe_3Pt phase.

To confirm the temperature-induced phase transition, XRD patterns of the $\text{Fe}_{80}\text{Pt}_{20}$ alloy in states A and B were measured, as shown in Fig. 2. State A was obtained by cooling from 950 to 300 K, while state B was obtained by heating from 5 to 300 K, as shown in Fig. 1. It can be seen that the $\text{Fe}_{80}\text{Pt}_{20}$ alloy in state A has a γ phase with a fcc structure, while it transformed to α phase with a bcc structure in state B. According to Rietveld refinement on the XRD patterns, the values of lattice parameter a of the γ phase and α phase are 3.7131 and 2.9417 Å, respectively. The change of a reaches 26.2% which is unusually high. In FeRh and Gd-SiGe alloys, the volume changes $|\Delta V/V|$ during the phase transitions, which is responsible for their giant magnetic entropy change, are only 0.9% and 0.4%, respectively.^{11,12} It is also very interesting to note that the phase transition from the γ phase to the α phase leads to broadened XRD peaks. This should be attributed to microstrain caused by the large lattice shrinkage in the polycrystalline materials. The inset of Fig. 2 gives the Williamson-Hall analysis of the XRD patterns.¹³ It

^{a)}Electronic mail: crong@uta.edu

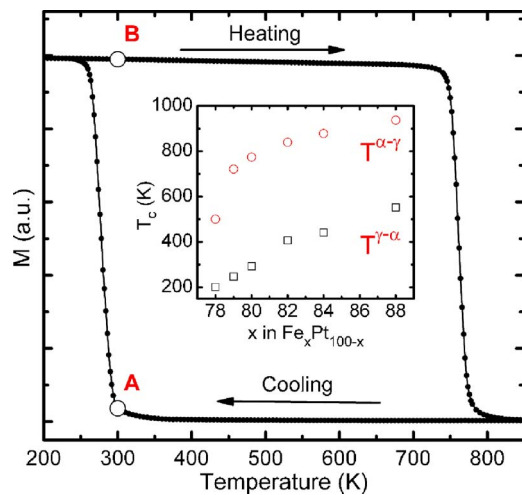


FIG. 1. (Color online) Thermomagnetic curves of the $\text{Fe}_{80}\text{Pt}_{20}$ alloy under 100 Oe magnetic field. The inset gives the dependence of $T^{\alpha\rightarrow\gamma}$ and $T^{\gamma\rightarrow\alpha}$ on x in $\text{Fe}_x\text{Pt}_{100-x}$ alloys.

shows that the slope of the Williamson-Hall plot in state B is much larger than that of state A, indicating a much higher microstrain in state B than that of state A in the $\text{Fe}_{80}\text{Pt}_{20}$ alloy. A quantitative analysis shows that the microstrain values in states A and B are $(0.1\pm 0.02)\times 10^{-3}$ and $(14.7\pm 2.1)\times 10^{-3}$, respectively.

Figure 3 shows the magnetization curves of the $\text{Fe}_{80}\text{Pt}_{20}$ alloy at different temperatures after cooling down from 950 to 350 K at a rate of 10 K/min. It shows that the alloys are paramagnetic when the temperature is higher than 310 K. At relatively low temperatures, magnetization hysteresis was observed. The magnetization increased fast when the magnetic field was higher than 4 T in the increasing field mode. This behavior is similar to the observations in MnFePAs and GdSiGe alloys where first-order phase transitions were observed.⁵ However, the fact that the magnetization curves with decreasing field do not go back to the starting points with increasing field even at zero field means that the mag-

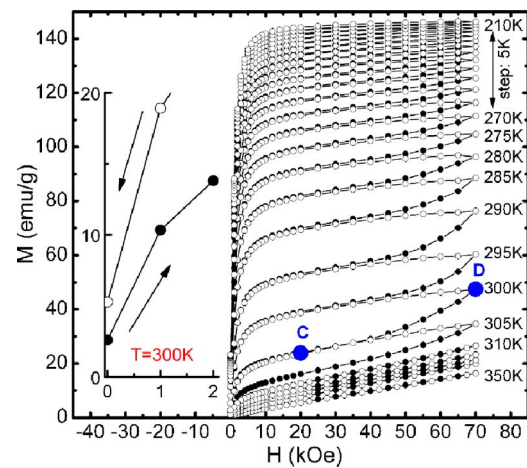


FIG. 3. (Color online) Isothermal M - H curves of the $\text{Fe}_{80}\text{Pt}_{20}$ alloy at different temperatures. The solid and open symbols represent the magnetization with increasing and decreasing magnetic fields, respectively. The inset gives the magnetizations near zero fields at 300 K by increasing and decreasing fields.

netic field induced phase transition is not reversible in the FePt alloys. The inset is an example at 300 K. It shows that the remanence magnetizations before and after applying 7 T magnetic field are 2.6 and 5.3 emu/g, respectively. Thus the induced structural phase transition content from γ to α is estimated to be around 11.6% by comparing with the remanence (23.2 emu/g) of the complete α phase at 210 K.

To understand the magnetic-field-induced structural phase transition, the XRD patterns of the $\text{Fe}_{80}\text{Pt}_{20}$ alloys corresponding to states C and D were measured (Fig. 4), as shown in Fig. 3. Both states C and D have the same thermal and magnetization histories, as shown by the M - H curves, i.e., the state C was obtained by increasing magnetic field to 2 T and then removing the field, while state D was obtained by applying a magnetic field of 7 T and then removing the field at 300 K. The XRD patterns were collected at room temperature and the intensity of peaks was normalized by the (111) peak of γ phase for comparison. It is found that in both

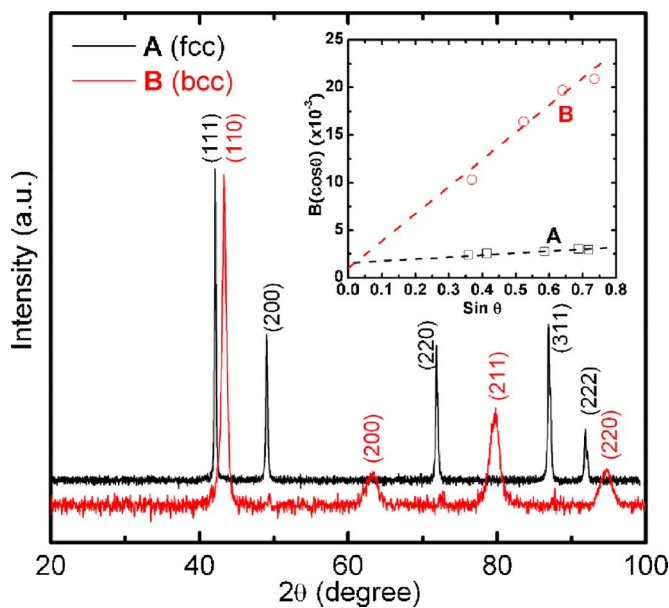


FIG. 2. (Color online) XRD patterns of the $\text{Fe}_{80}\text{Pt}_{20}$ alloy in states A and B of Fig. 1. The inset gives the Williamson-Hall plots of $\text{Fe}_x\text{Pt}_{100-x}$ ($x=80$) alloy in different states.

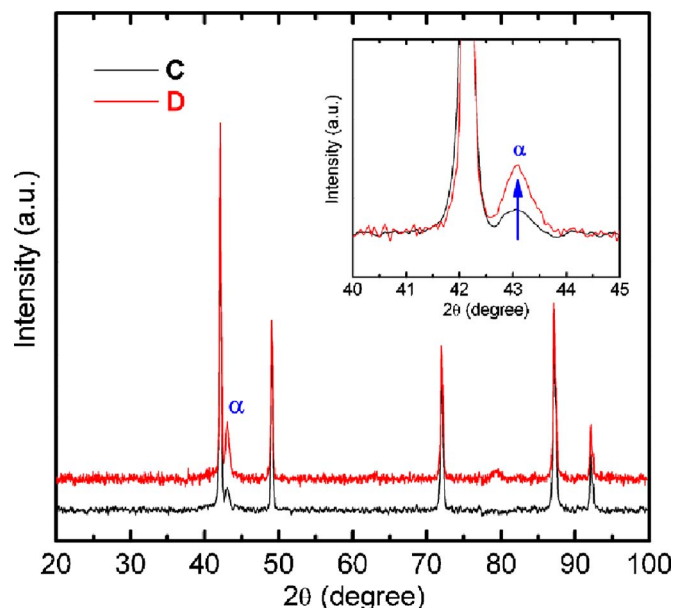


FIG. 4. (Color online) XRD patterns of the $\text{Fe}_{80}\text{Pt}_{20}$ alloy in states C and D. The inset gives the enlarged patterns focused in $2\theta=40-45^\circ$.

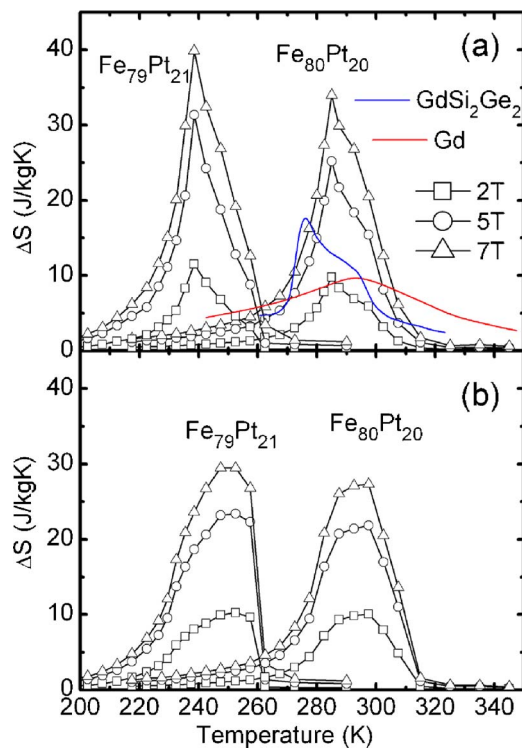


FIG. 5. (Color online) Magnetic entropy change $|\Delta S|$ of $\text{Fe}_{79}\text{Pt}_{21}$ and $\text{Fe}_{80}\text{Pt}_{20}$ alloys for the magnetic field changes of 0–2, 0–5, and 0–7 T with (a) increasing field and (b) decreasing field, respectively. For comparison, the $|\Delta S|$ of Gd and $\text{Gd}_5\text{Ge}_2\text{Si}_2$ under 0–5 T are also presented which are quoted from Refs. 6 and 7.

states there exists a mixture of γ and α phases. However, the peak intensity of the α phase in state D is higher than that in state C (as shown in the inset of Fig. 4), which means that the content of α phase in state D is higher than that in state C. A quantitative analysis shows that the contents of α phase in state C and D are 8.7% and 20.4%, respectively. This is consistent with the analysis of remanence magnetization as discussed above. Thus, it can be concluded that the high magnetic field also can induce the structural phase transition from the γ phase to the α phase. It is noted that there was no α phase in the alloy under zero or low field at room temperature (state A in Fig. 2), while at state C (2 T, room temperature) the peaks from the α phase showed up. This should be attributed to the phase transition during the high-field magnetic measurement at 305 K, as shown in Fig. 3.

Figure 5(a) gives the magnetic entropy change $|\Delta S|$ obtained by the Maxwell relation^{14–16} of the alloys with $x=79$ and 80 by increasing field. The calculated maximum values of $|\Delta S|$ under field changes from 0 to 5 T are 31.3 and 25.2 J/kg K for the alloys with $x=79$ and 80, respectively. These values are far higher than those of Gd (9.7 J/kg K) and $\text{Gd}_5\text{Si}_2\text{Ge}_2$ (18.6 J/kg K).^{6,7} The maximum $|\Delta S|$ values can be improved to 39.8 and 34.0 J/kg K under the field change of 0–7 T for the alloys with $x=79$ and 80, respectively. Such large $|\Delta S|$ values were rarely observed in the Gd systems at the corresponding temperatures. The origin of GMCE in the present FePt alloys can be attributed to the coupled temperature- and field-induced structural phase transition. The huge negative lattice expansion in FePt alloys

during the phase transition should be the reason for the giant $|\Delta S|$ values.

As discussed in Fig. 3, an increasing field can induce the $\gamma \rightarrow \alpha$ phase transition, while it is not reversible with a decreasing field. Hence we can estimate the contribution of a field induced structural phase transition on GMCE by comparison of the $|\Delta S|$ values upon increasing and decreasing field measurements. Figure 5(b) gives $|\Delta S|$ under different fields for the decreasing field measurements. The maximum values of $|\Delta S|$ were around 29.5 and 27.3 J/kg K under 0–7 T for the alloys with $x=79$ and 80, respectively. It is noted that the $|\Delta S|$ peak with increasing field is sharper than that with decreasing field since the magnetic-field-induced structural phase transition concentrates the magnetic entropy change to a narrow temperature range. By comparison of Figs. 5(a) and 5(b), the contributions of field induced structural phase transition on GMCE are estimated to be around 10.3 and 6.7 J/kg K (25% and 20% of the total $|\Delta S|$) for the alloys with $x=79$ and 80, respectively.

In summary, in the $\text{Fe}_x\text{Pt}_{100-x}$ ($x=78–88$) alloys a structural phase transition from disordered γ phase to the ordered α phase was observed during cooling, and a reverse process takes place during heating. Moreover, a magnetic field induces the structural phase transition from the γ phase to the α phase near the transition temperature. The temperature- and magnetic-field-induced first-order phase transition lead to a huge negative thermal expansion (around 26.2%), and thus giant magnetic entropy changes of 39.8 and 34.0 J/kg K for the alloys with $x=79$ and 80, respectively. This large entropy change may be useful for magnetocaloric material applications. However, elimination of the thermal hysteresis (e.g., by element doping) is necessary for potential applications.

This work was supported by U.S. DoD/MURI Grant No. N00014-05-1-0497 and DARPA through ARO under Grant No. DAAD 19-03-1-0038.

¹M. Hansen, *Metallurgy and Metallurgical Engineering Series, Constitution of Binary Alloys* (McGraw-Hill, New York, 1958), pp. 698–700.

²A. Kussmann and G. V. Rittberg, *Z. Metallkd.* **452**, 470 (1950).

³A. E. Berkowitz, F. J. Donahoe, A. D. Franklin, and R. P. Steijn, *Acta Metall.* **5**, 1 (1957).

⁴C. B. Rong, Y. Li, and J. P. Liu, *J. Appl. Phys.* **101**, 09K505 (2007).

⁵S. A. Nikitin, G. Myalikgulyev, M. P. Annaorazov, A. L. Tyurin, R. W. Myndyev, and S. A. Akopyan, *Phys. Lett. A* **171**, 234 (1992).

⁶V. K. Pecharsky and K. A. Gschneidner, *Phys. Rev. Lett.* **78**, 4494 (1997).

⁷F. X. Hu, B. G. Shen, J. R. Sun, G. J. Wang, and Z. H. Cheng, *Appl. Phys. Lett.* **80**, 826 (2002).

⁸O. Tegus, E. Brück, K. H. Buschow, and F. R. de Boer, *Nature (London)* **415**, 150 (2002).

⁹O. Tegusa, E. Bruck, L. Zhang, Dagula, K. H. J. Buschow, F. R. de Boer, *Physica B* **319**, 174 (2002).

¹⁰K. A. Gschneidner, Jr., V. K. Pecharsky, and A. O. Tsokol, *Rep. Prog. Phys.* **68**, 1479 (2005).

¹¹P. A. Algarabel, M. R. Ibarra, C. Marquina, A. D. Moral, J. Galibert, M. Iqbal, and S. Askenazy, *Appl. Phys. Lett.* **66**, 3061 (1995).

¹²L. Morellon, P. A. Algarabel, M. R. Ibarra, J. Blasco, B. Garcia-Landa, Z. Arnold, and F. Albertini, *Phys. Rev. B* **58**, R14721 (1998).

¹³K. Williamson and W. H. Hall, *Acta Metall.* **1**, 22 (1953).

¹⁴V. K. Pecharsky and K. A. Gschneidner, Jr., *J. Appl. Phys.* **86**, 565 (1999).

¹⁵J. R. Sun, F. X. Hu, and B. G. Shen, *Phys. Rev. Lett.* **85**, 4191 (2000).

¹⁶G. J. Liu, J. R. Sun, J. Shen, B. Gao, H. W. Zhang, F. X. Hu, and B. G. Shen, *Appl. Phys. Lett.* **90**, 032507 (2007).